

HEAT/MASS TRANSFER IN TAYLOR VORTEX FLOW WITH CONSTANT AXIAL FLOW RATES

K. KATAOKA,* H. DOI† and T. KOMAI‡

Department of Chemical Engineering, Kobe University, Kobe, Japan

(Received 19 April 1976)

Abstract—An experimental investigation was done by the use of electrochemical technique in order to obtain the interrelation between the axial movement of Taylor vortices and the periodically varying rates of heat/mass transfer on the internal surface of the outer cylinder. When the Reynolds number of the axial flow is raised gradually at a fixed value of the Taylor number of the rotating flow, the regular sinusoidal variation of Sherwood numbers is distorted by the axial flow added, and then its mean value and amplitude are greatly reduced. The axial flow causes the damping effect not only on the initial formation of Taylor vortices but also on the heat/mass transfer mechanism involved in the momentum vortex boundary layer. It has been found that application of the heat-transfer data obtained for zero axial flow rate in order to design this type of heat exchanger with small, constant axial flow leads to dangerous 30–50% underestimation of the surface area of heat transfer in the experimental range.

NOMENCLATURE

C_b , bulk concentration [mol/m³];
 C_w , concentration at the outer cylinder surface [mol/m³];
 D , diffusivity [m²/s];
 d , gap width between two coaxial cylinders [m];
 k , mass-transfer coefficient on the internal surface of outer cylinder, $k = N/(C_b - C_w)$, [m/s];
 N , mass flux on the internal surface of outer cylinder [mol/m² s];
 n , integer;
 Re , Reynolds number, $2\langle w \rangle d/v$;
 R_i , inner cylinder radius [m];
 r, θ, z , cylindrical coordinates [m, -, m];
 Sc , Schmidt number, v/D ;
 Sh , Sherwood number, $2kd/D$;
 T , periodic time required for a couple of Taylor vortices to pass by a point in axial direction [s];
 Ta , Taylor number, $(R_i \omega d/v)(d/R_i)^{1/2}$;
 t , time [s];
 u, v, w , velocity components in cylindrical coordinate system [m/s, m/s, m/s].

$'$, disturbance with respect to z ;
 l , amplitude of velocity disturbance;
 $\langle \rangle$, average over the cross-section of the annulus.

INTRODUCTION

THE PRESENT paper is an investigation of the transport phenomena which control the rate of heat/mass transfer in an annulus formed by two concentric cylinders with rotation of the inner cylinder. From an engineering view point, the heat-transfer phenomena in the annulus become very important, especially when the fluid possesses an independent axial motion because problems of this type may arise in the design and operation of chemical engineering process equipment as well as rotating machinery.

In this flow system, the modes of flow can be characterized as a function of two independent dimensionless parameters: Taylor number of the rotating motion and Reynolds number of the axial motion. When the Taylor number exceeds a critical value for no axial flow, there appear pairs of counter-rotating toroidal vortices regularly spaced along the axis, surrounding the inner cylinder like a vortex ring. When a small, constant axial flow is added in such a vortex motion, each vortex marches through axially in single file without breaking up. It has been found in the previous work [1] that such a flow system can be an ideal plug-flow. Figure 1 shows this flow pattern and the coordinate system.

Although considerable information [2–5] has been published on the over-all heat-transfer coefficients in annuli for no axial flow, few heat-transfer data are available for the case when a constant axial flow is added. The significant studies found were those of Becker and Kaye [6] on the diabatic flow and of Astill [7] on the developing adiabatic flow. However, only the former tried to correlate the over-all coefficients of heat transfer with Taylor number and Reynolds number because of difficulties in the measure-

Greek symbols

Δ , wavelength [m];
 λ , wave-number [1/m];
 ν , kinematic viscosity [m²/s];
 ω , angular velocity of inner cylinder [1/s].

Superscripts, Subscripts and Bracket

—, average with respect to z or t ;
 $\overline{\quad}$, average with respect to z and t ;

*Associate Professor of Chemical Engineering, Kobe University, Kobe 657, Japan.

†Chemical Engineer, Hitachi Shipbuilding Co., Ltd., Osaka 554, Japan.

‡Graduate Student, Kobe University, Kobe 657, Japan.

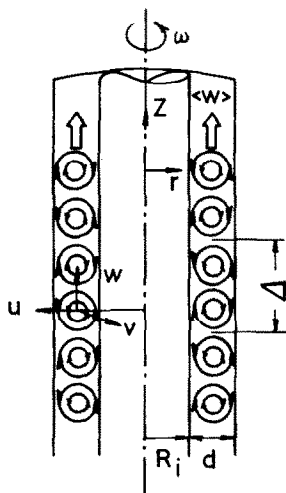


FIG. 1. Flow configuration of Taylor system of vortices moving axially and the cylindrical coordinate system.

ment of locally and temporally varying rates of heat transfer to each cylinder surface. Much yet remains to be done as to how the Taylor vortex motion controls the momentum vortex boundary layer where heat/mass transfer takes place.

The main purpose of the present work is to observe the interrelation between the axial movement of Taylor vortices and the periodically varying rates of mass transfer by measuring simultaneously the local coefficients of mass transfer on the internal surface of the outer cylinder and the fluid motion of the axially moving Taylor vortices. The experiments have been conducted with the aid of electrochemical technique [8, 9] under the assumption of analogy between heat and mass transfer. Measurements can be regarded as those of heat transfer to a constant-temperature wall from a fluid of large Prandtl number.

EXPERIMENTS

The general arrangement of the apparatus is shown schematically in Fig. 2.

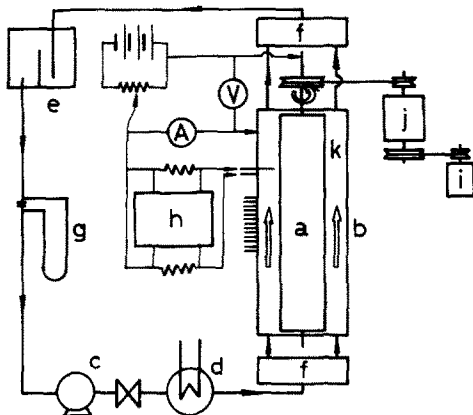


FIG. 2. General arrangement of the apparatus. (a) inner rotating cylinder, (b) outer stationary cylinder, (c) pump, (d) heat exchanger, (e) tank, (f) mixing box, (g) flow meter, (h) two-channel analog recorder/oscillograph, (i) motor, (j) vari-speeder, (k) test section (annulus).

The test section of the apparatus is similar to that used in the previous studies [10, 11], except that it was modified chiefly by changes in the inlet and outlet section for supplying a constant, uniform axial flow and by insertion of three wire cathodes into the annulus for observing the axially moving Taylor vortices.

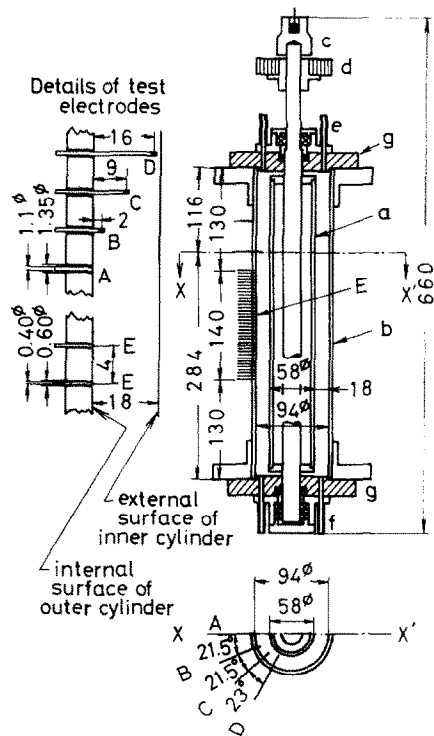


FIG. 3. Test section of apparatus and the details of test cathodes. Dimensions given are in mm. (a) inner rotating cylinder, (b) outer stationary cylinder, (c) mercury well, (d) driving gear, (e) outlet pipe, (f) inlet pipe, (g) bakelite flange, A,B,C,D,E test cathode.

Figure 3 shows the details of the test section, which comprises two concentric vertical cylinders. The inner cylinder, turned from a copper pipe, is 380 mm long, with an O.D. of 58.0 mm. The outer cylinder with an I.D. of 94.0 mm was fabricated by honing the inside surface of copper pipe. The annulus formed by two cylinders is 18.0 mm wide, 380 mm long. The inner copper cylinder used as the anode is supported at each end by bearing-oil-seal assembly and is driven by a motor. The outer copper cylinder used as the main cathode contains two types of test cathodes: thirty-six 0.4-mm-dia circular copper cathodes (Type E) embedded axially every 4 mm on the outer cylinder surface for measurement of the local rates of mass transfer in the case when the inner cylinder is rotated with zero axial flow rate and a 1.1 mm-dia circular copper cathode (Type A) embedded at 284 mm from the bottom on the outer cylinder surface for measurement of the rates of mass transfer in the general case when the inner cylinder is rotated with constant axial flow rates. In addition, three 1.1 mm-dia copper wire cathodes (Type B, C, D) were inserted into the annulus and placed at the same horizontal level at 284 mm from the bottom and

they were separated in arc by approximately 20° , respectively. As shown in Fig. 3, these wire cathodes B, C, D have an active surface, respectively, at approximately 2 mm from the outer cylinder surface, 9 mm (center of the annulus), and 2 mm from the inner cylinder surface. This type of wire cathodes are very sensitive to the velocity components (i.e. v and w) perpendicular to the cathode surface but not very sensitive to the radial velocity component (i.e. u) parallel to the cathode surface.

The working fluid and the experimental conditions are shown in Table 1. The fluid is fed into the annulus at a constant axial flow rate through three 8.5 mm-dia inlet holes of the bottom flange, being exhausted through three 8.5 mm-dia outlet holes of the top flange.

Table 1. Working fluid and experimental conditions

Electrolytic aqueous solution	CuSO ₄ [mol/m ³] H ₂ SO ₄ [mol/m ³] Glycerin [wt%]	1.15–1.75 2×10^3 0–58.4
Ta		35–9200
Re		0–260
Sc		3×10^3 – 8×10^5
v [m ² /s]		1.3×10^{-6} – 13×10^{-6}

The rates of mass transfer on the internal surface of the outer cylinder are measured by measuring the current discharged to the test cathodes (Type A, E) under the limiting current condition. It was ascertained by the earlier work [12] that the critical Taylor number was approximately 60 with zero axial flow rate for the present geometry $d/R_i = 0.62$. All data were taken under isothermal conditions.

EXPERIMENTAL RESULTS AND DISCUSSION

I. Local coefficient of mass transfer

Case A: Taylor vortex flow with zero axial flow rate. The axial variation of local mass-transfer coefficients measured with Type E electrodes is shown in Figs. 4 and 5, in which the axial distance coordinate was made dimensionless by using a wave-length of a couple of vortices Δ as the reference length.

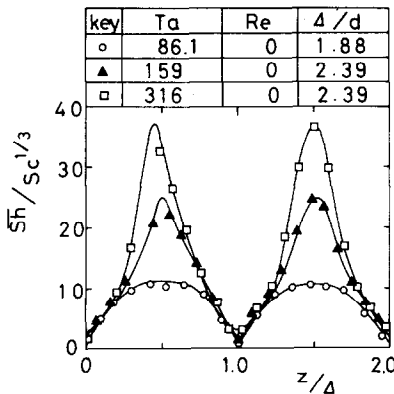


FIG. 4. Axial variation of local mass-transfer coefficients in the case of Taylor vortex flow with zero axial flow rate.

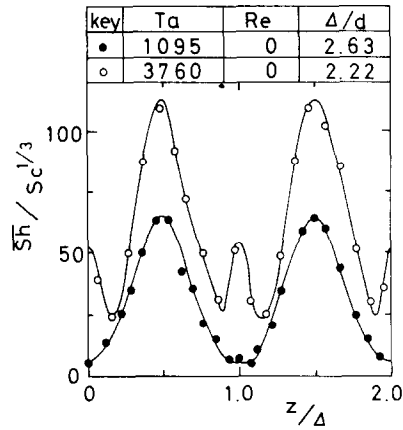


FIG. 5. Axial variation of local mass-transfer coefficients in the case of Taylor vortex flow with zero axial flow rate.

It can be seen that the local Sherwood numbers show a remarkable sinusoidal periodicity in axial direction as the result of the axial arrangement of Taylor vortices, except for their cycloidal periodicity in a very short supercritical range of Taylor number. At $Ta > 1000$, the local Sherwood numbers show a new secondary peak at the back-flow section of secondary flow.

Case B: Taylor vortex flow with constant axial flow rates. The data were taken close together at a fixed value of Taylor number as the Reynolds number was varied to detect any changes which might occur in the flow pattern in the annulus. The results were obtained in that section of the test apparatus where the concentration and velocity boundary layers were fully developed, both radially and axially. Even when the Reynolds number was very large within the experimental range, no appreciable difference in the shape and amplitude could be found between two curves of mass transfer rate measured at any two measuring points except for a phase-shift caused by the distance-velocity lag.

The temporal variation of local mass-transfer coefficients measured with Type A electrode at one measuring point is shown in Figs. 6–8, in which the

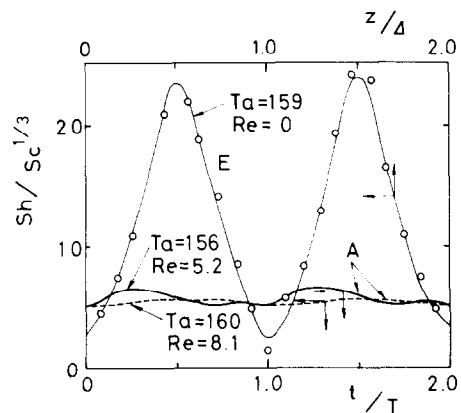


FIG. 6. Temporal variation of mass-transfer coefficients in the case of Taylor vortex flow with different axial flow rates.

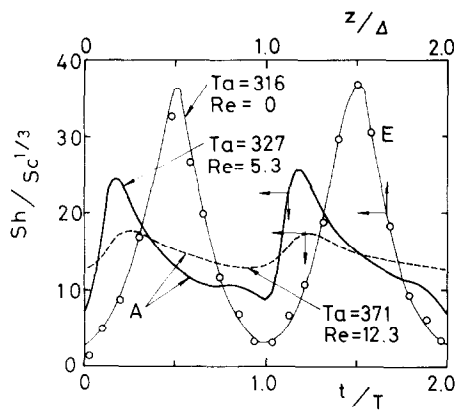


FIG. 7. Temporal variation of mass-transfer coefficients in the case of Taylor vortex flow with different axial flow rates.

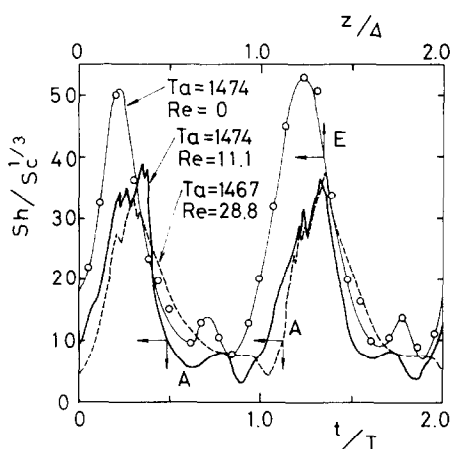


FIG. 8. Temporal variation of mass-transfer coefficients in the case of Taylor vortex flow with different axial flow rates.

time coordinate was also made dimensionless by using the periodic time T required for a couple of vortices to axially pass by the measuring point as the reference time. It should be noted that as the Reynolds number is raised gradually, the regular sinusoidal variation of Sherwood numbers is not only distorted by the axial motion but also its mean value and amplitude are greatly reduced. The axial motion can be considered to cause the damping effect on the initial formation of Taylor vortices or to increase stability of the laminar flow. This tendency depends upon the relative magnitude between the Taylor number and Reynolds number.

II. Interrelation between the local rates of mass transfer and the axial movement of Taylor vortices

Taylor vortex flow of this type can be assumed to have the following velocity components:

$$\begin{aligned} u &= u^* = u_1(r) \cos \lambda(z - \langle w \rangle t) \\ v &= v + v' = \bar{v}(r) + v_1(r) \cos \lambda(z - \langle w \rangle t) \\ w &= \langle w \rangle + w' = \langle w \rangle + w_1(r) \sin \lambda(z - \langle w \rangle t). \end{aligned}$$

Only in the above equations are all the quantities made dimensionless. Axial, constant velocity component was

assumed to be uniform over the cross-section of the annulus because the Taylor vortices, which had grown to their full extent, marched axially in single file through the annulus [1]. According to the measurements given by Mizushima *et al.* [12] for zero axial flow rate, it can be considered that \bar{v} is much larger than $v_1(r)$ and $v_1(r)$ is also much larger than $w_1(r)$ and $u_1(r)$, even in the vicinity of the outer cylinder. Besides, in the present experimental range $Re \ll Ta$, \bar{v} is much larger than $\langle w \rangle$. Because v' is in phase with u' , v' and u' show maxima and minima at the same phases. Therefore, the current discharged to the wire cathodes (Type B, C, D) should also show maxima at the jet section of the secondary flow [i.e. $\lambda(z - \langle w \rangle t) = 2n\pi$] and minima at the back-flow section [i.e. $\lambda(z - \langle w \rangle t) = (2n+1)\pi$].

Figures 9 and 10 show a schematic picture of the Taylor vortices distorted by the axial motion in correspondence with the temporal variations of the mass-transfer coefficients measured with Type A electrode and of the currents of three wire cathodes Type B, C, D. (Each symbol was used to emphasize the correspondence. The reversal of magnitude of the currents discharged to Type C, D electrodes in Fig. 10 is due to the fact that the electrode surface area of Type C was larger than that of Type D.) According to Snyder *et al.* [13], the back flow becomes slow and occupies most of the cell, whereas the jet is formed at the cell boundary and is always outward from the inner rotating cylinder. It appears that the jet exerts a great effect on the mass transfer to the outer stationary cylinder at the point of impact.

When Re is raised gradually at $Ta = 694$, the current of the wire cathode placed near the inner rotating cylinder shows small random oscillation superimposing the main periodic change and a small secondary peak at the minimum section. Physically this means that a couple of small secondary vortices are formed at the back-flow section near the inner cylinder.

When $Ta = 2550$, three currents measured with Type B, C, D electrodes show remarkable periodic oscillation with the superimposing small random oscillation which characterizes turbulent flow. This turbulent vortex flow regime is similar to the turbulent vortex flow with no axial flow [10]. When Ta exceeds about 1000, the mass-transfer coefficients show a new secondary peak at the back-flow section of the secondary flow. It can be found from the current of the wire cathode (Type B) placed near the outer cylinder that the secondary peak indicates the generation of a new couple of small secondary vortices due to the separation of the boundary layer from the outer cylinder wall. Figure 11 shows the experimental flow conditions for the occurrence of different flow regimes. The transition from laminar vortex to turbulent vortex flow occurs gradually over the relatively wide range of Taylor number $Ta = 500 \sim 1000$. When $Re = 20$, for example, the laminar vortex flow regime, which has been established at $Ta = 100$, remains stable up to $Ta = 500$. At $Ta = 500$ the transition begins with the generation of disturbance near the inner rotating cylinder, accompanied with small secondary vortices there. When Ta

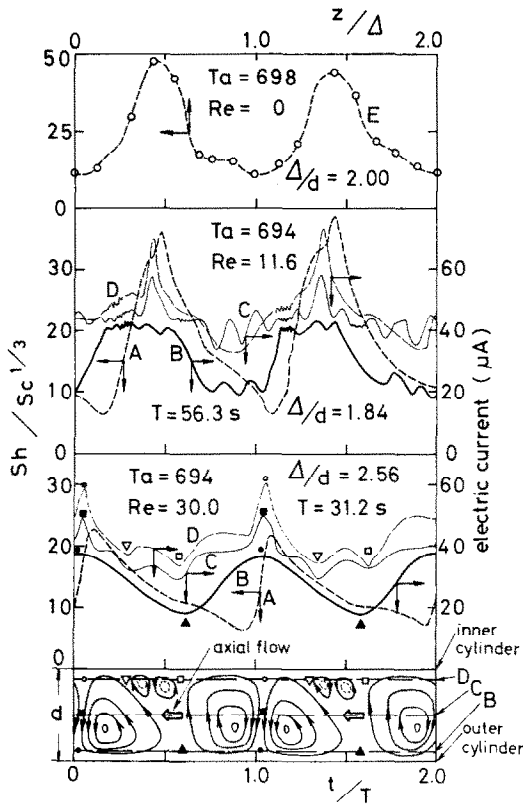


FIG. 9. Schematic picture of axially moving Taylor vortices.

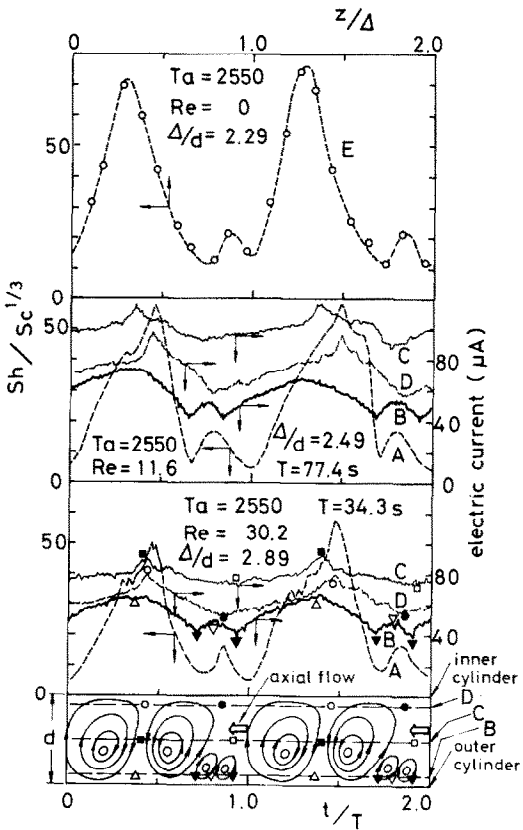


FIG. 10. Schematic picture of axially moving Taylor vortices.

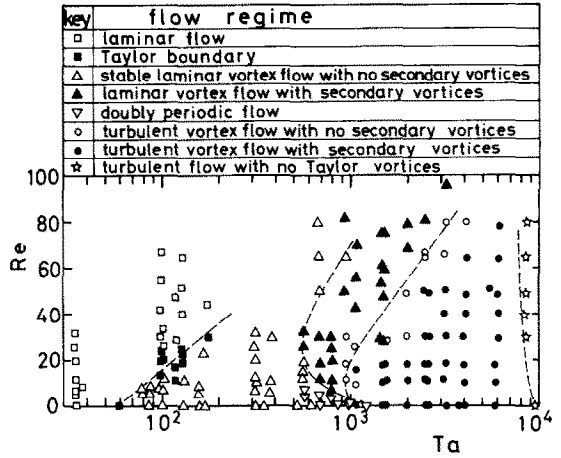


FIG. 11. Experimental flow conditions for the occurrence of different flow regimes.

exceeds 1000, the disturbance travels radially outward, so that the flow attains the turbulent vortex flow regime, followed by the formation of small secondary vortices near the outer stationary cylinder due to separation. At very low Reynolds numbers ($Re < 10$), the transition to turbulent vortex flow seems to proceed by way of the same doubly-periodic flow region as for no axial flow [14]. Figure 12 shows typical variation of the currents discharged to Type A, B, D electrodes in the doubly-periodic flow region. The currents

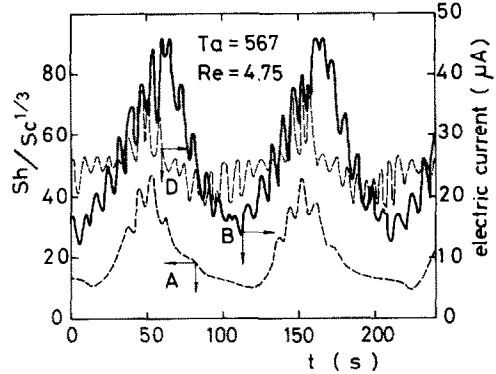


FIG. 12. Typical variation of electrode currents in doubly-periodic flow.

show the wavy oscillation that characterizes the azimuthal wavy structure of the doubly-periodic flow. On the other hand, it was difficult to clearly ascertain the transition at very high Reynolds numbers. It was also insignificant from the engineering view point of the present work. The above understanding of the transition should be limited within low Reynolds number range $0 < Re < 80$ because the structure of the test apparatus was inadequate to obtain high axial velocities.

Figure 13 shows the effect of the Reynolds number on the generation of Taylor vortices. When Re is small compared with Ta (e.g. when $Re < 20.3$ at $Ta = 101$), the remarkable periodic oscillation of the currents discharged to the wire cathodes B, D proves the existence

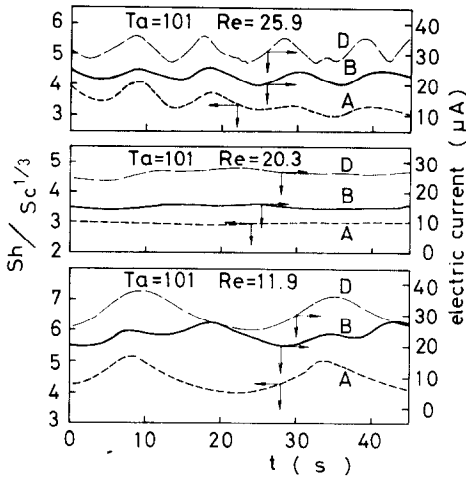


FIG. 13. Effect of Reynolds number on the generation of Taylor vortices.

of Taylor vortices and the rate of mass transfer is greatly enhanced due to non-linear mechanics of disturbances [3, 4, 11] in Taylor vortex flow. When Re becomes a critical value (e.g. when $Re = 20.3$ at $Ta = 101$), the currents of the wire cathodes cease to show any periodic oscillation. It is found that the Taylor vortices disappear just at the Reynolds number. When Re is large compared with Ta (e.g. when $Re > 20.3$ at $Ta = 101$), the currents again seem to have small periodic oscillation. However, the recorder

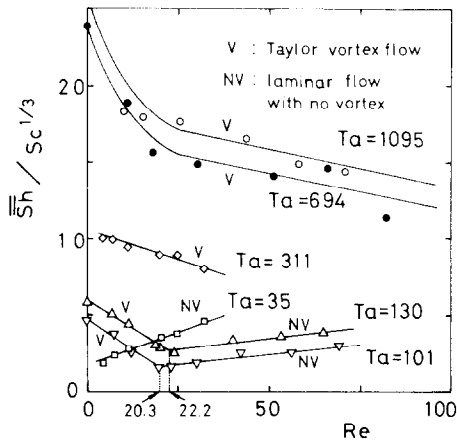


FIG. 14. Effect of Reynolds number on the average Sherwood number.

traces of velocity disturbance do not come from the stable Taylor vortex motion because no appreciable increase in mass transfer, which characterizes the non-linear interaction of disturbances of Taylor vortex flow, can be found. In other words, as shown in Fig. 14, \bar{Sh} increases with increasing Re when the flow is purely laminar, whereas \bar{Sh} decreases with increasing Re as long as the Taylor vortices exist.

These phenomenological results are quite interesting for the study of the heat-transfer mechanism involved in the momentum vortex boundary layer.

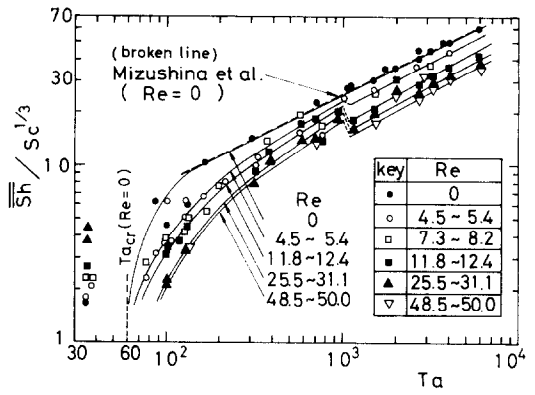


FIG. 15. Average Sherwood number vs Taylor number.

III. Average mass-transfer coefficient

Figure 15 shows the average mass-transfer coefficients in terms of Taylor number and Reynolds number. It is found that \bar{Sh} increases with increasing Ta but decreases with increasing Re as long as the Taylor vortices exist. The axial motion causes the damping effects not only on the Taylor instability but also on the mass transfer. It can be seen from Fig. 15 that if the heat-transfer data obtained for zero axial flow rate are used for the design calculation of this type of heat exchanger with axial flow, it leads to 30–50% underestimation of the surface area for heat transfer. It is also found that the damping effect of the axial flow i.e. Re on \bar{Sh} is greater in the turbulent vortex flow region ($Ta > 1000$) than in the laminar vortex flow region ($Ta < 1000$). The reason for the two distinct damping effects was carefully examined but no satisfactory explanation was found.

CONCLUSION

When no axial flow is added to Taylor vortex flow, the local Sherwood numbers show a remarkable sinusoidal periodicity in axial direction. When Reynolds number of the axial motion is raised gradually, the regular sinusoidal variation of Sherwood numbers is not only distorted but also its mean value and amplitude are greatly reduced by the axial flow added. The axial motion causes the damping effects on the initial formation of Taylor vortices and the mass-transfer mechanism involved in the momentum vortex boundary layer. As long as the Taylor vortices exist, the average Sherwood number increases with increasing Taylor number but decreases with increasing Reynolds number. Application of the heat-transfer data for zero axial flow rate in order to design this type of heat exchanger leads to dangerous 30–50% underestimation of the surface area for heat transfer.

REFERENCES

1. K. Kataoka, H. Doi and T. Hongo, Ideal plug-flow properties of Taylor vortex flow, *J. Chem. Engng. Japan* **8**, 472–476 (1975).
2. I. S. Bjorklund and W. M. Kays, Heat transfer between concentric rotating cylinders, *J. Heat Transfer* **81C**, 175–186 (1959).

3. C. Y. Ho, J. L. Nardacci and A. H. Nissan, Heat transfer characteristics of fluids moving in a Taylor system of vortices, *A.I.Ch.E. Jl* **10**, 194–202 (1964).
4. H. Aoki, H. Nohira and H. Arai, Convective heat transfer in an annulus with an inner rotating cylinder, *Bull. J.S.M.E.* **10**, 523–532 (1967).
5. T. Mizushima, R. Ito, T. Nakagawa, K. Kataoka and S. Yokoyama, Turbulent momentum and heat transfer in an annulus between rotating coaxial cylinders, *Kagaku-Kogaku (Chem. Engng. Japan)* **31**, 974–980 (1967).
6. K. M. Becker and J. Kaye, Measurements of diabatic flow in an annulus with an inner rotating cylinder, *J. Heat Transfer* **84C**, 97–105 (1962).
7. K. N. Astill, Studies of the developing flow between concentric cylinders with the inner cylinder rotating, *J. Heat Transfer* **86C**, 383–392 (1964).
8. T. J. Hanratty, Study of turbulence close to a solid wall, *Physics Fluids Suppl.* S126–S133 (1967).
9. T. Mizushima, The electrochemical method in transport phenomena, in *Advances in Heat Transfer*, Vol. 7, pp. 87–161. Academic Press, New York (1971).
10. T. Mizushima, R. Ito, K. Kataoka, S. Yokoyama, Y. Nakashima and A. Fukuda, Transition of flow in the annulus of concentric rotating cylinders, *Kagaku-Kogaku (Chem. Engng. Japan)* **32**, 795–800 (1968).
11. K. Kataoka, Heat-transfer in a Taylor vortex flow, *J. Chem. Engng. Japan* **8**, 271–276 (1975).
12. T. Mizushima, R. Ito, K. Kataoka, Y. Nakashima and A. Fukuda, Velocity distributions of Taylor vortex flow in an annulus between rotating coaxial cylinders, *Kagaku-Kogaku (Chem. Engng. Japan)* **35**, 1116–1121 (1971).
13. H. A. Snyder and R. B. Lambert, Harmonic generation in Taylor vortices between rotating cylinders, *J. Fluid Mech.* **26**, 545–562 (1966).
14. D. Coles, Transition in circular Couette flow, *J. Fluid Mech.* **21**, 385–425 (1965).

TRANSFERT DE CHALEUR ET DE MASSE DANS UN ECOULEMENT TOURBILLONNAIRE DE TAYLOR AVEC VITESSE AXIALE CONSTANTE

Résumé—Une étude expérimentale a été effectuée à l'aide d'une méthode électrochimique dans le but de déterminer la relation entre le mouvement axial des tourbillons de Taylor et les taux périodiques de transfert de chaleur et de masse sur la surface interne du cylindre extérieur. Lorsque le nombre de Reynolds de l'écoulement axial est augmenté progressivement en maintenant constant le nombre de Taylor de l'écoulement circulaire, les variations sinusoidales régulières du nombre de Sherwood sont perturbées par l'écoulement axial superposé et il en résulte une nette diminution de sa valeur moyenne et de son amplitude. L'amortissement provoqué par l'écoulement axial s'applique non seulement à la formation des tourbillons de Taylor mais aussi au mécanisme de transfert de chaleur et de masse agissant dans la couche limite du tourbillon. Il est apparu que l'application des données de transfert thermique obtenues dans des conditions de vitesse axiale nulle, dans le but de dimensionner ce type d'échangeur de chaleur avec vitesse axiale constante et faible, conduit à une dangereuse sous-estimation de 30–50% de la surface de transfert, dans le domaine expérimental exploré.

WÄRME- UND STOFFAUSTAUSCH IN TAYLOR-STRÖMUNGEN MIT KONSTANTEN AXIALEN STRÖMUNGSDURCHSÄTZEN

Zusammenfassung—Mit Hilfe der elektrochemischen Technik wurde eine experimentelle Untersuchung des Zusammenhangs zwischen der axialen Bewegung von Taylor-Wirbeln und dem periodisch sich ändernden Wärme- und Stoffaustausch auf der Innenseite des äußeren Zylinders durchgeführt. Wird die Reynolds-Zahl der Axialströmung bei konstanter Taylor-Zahl der Rotationsströmung allmählich erhöht, so erfährt die üblicherweise sinusförmige Veränderung der Sherwood-Zahlen durch die aufgezwungene Axialströmung eine Verzerrung, und die mittlere Sherwood-Zahl sowie deren Amplitude werden stark reduziert. Der durch die Axialströmung verursachte Dämpfungseffekt wirkt sich nicht nur auf die anfängliche Bildung der Taylor-Wirbel, sondern auch auf den Wärme- und Stoffaustausch-Mechanismus in der Impulswirbelgrenzschicht aus. Es zeigte sich, daß die Anwendung der bei nicht vorhandener Axialströmung ermittelten Wärmeübergangswerte auf die Auslegung von Wärmeübertragern mit kleinen, konstanten Axialströmungen zu einer gefährlichen Unterdimensionierung von etwa 30–50% im experimentell untersuchten Bereich führt.

ТЕПЛО- И МАССОБМЕН В ПОТОКЕ ВИХРЕЙ ТЕЙЛОРА ПРИ ПОСТОЯННЫХ АКСИАЛЬНЫХ РАСХОДАХ

Аннотация — С помощью электрохимического метода проводилось экспериментальное определение зависимости между аксиальным движением вихрей Тейлора и периодически изменяющимися скоростями тепло- и массообмена на внутренней поверхности наружного цилиндра. При постепенном увеличении числа Рейнольдса аксиального потока, при фиксированном значении числа Тейлора для вращающегося потока, регулярное синусоидальное изменение числа Шервуда нарушается благодаря аксиальному течению, а затем происходит сильное уменьшение его среднего значения и амплитуды. Аксиальное течение вызывает не только снижение амплитуды первоначально образующихся вихрей, но и ослабляет механизм тепло/массообмена в прандтлевском пограничном слое. Найдено, что применение данных по теплообмену, полученных для нулевого аксиального расхода, при расчете теплообменников этого типа с небольшим постоянным аксиальным потоком приводит к нежелательному занижению на 30–50% площади поверхности теплообмена в диапазоне изменения экспериментальных данных.